A COMPUTER CONTROLLED TYPE-2 TELEMETRY TRACKING SYSTEM

Michael James Hart
STEWS-ID-DT
White Sands Missile Range
WSMR, New Mexico 88002

ABSTRACT

The seven WSMR Transportable Telemetry Acquisition Systems (TTAS), have served WSMR well as primary telemetry tracking systems since their acquisition over twenty years ago. Increasing maintenance demands for the original analog position control system (the antenna feed, servo power amplifiers, and position compensation) coupled with the potential for substantial tracking system performance improvement and self-diagnostic capability offered by current technology led to the establishment of a new instrumentation development task at WSMR whose objective was the development of a new, almost totally digital prototype tracking system to replace the aging analog control system in one of the TTAS's. A modern conical scan feed has replaced the original monopulse feed, pulse-width-modulated power amplifiers have replaced the originals using SCR's, and a VMEbus-based computer using a real-time operating system has replaced the analog compensation and overall control of the system.

In this paper, following an overview of the prototype tracking system, the results of the development of a new position control algorithm for the prototype tracking system are described using root loci, computer simulation, and from the actual tracking system using servo test software developed for the computer controller. The results of the study of the old analog control system using computer simulation are presented for comparison. Problems encountered with the TTAS directly affecting position control are also presented.

The new position control algorithm was designed to accommodate all of the critical tracking system

nonlinearities (power amplifier saturation, current limiting, dead band, and control output saturation), all tracking modes (autotrack, manual, and using external pointing data), different operating bandwidths, and all possible drive inputs to the system. It has converted the tracking system from a type-1 to a type-2 control system improving the dynamic capability of the TTAs.

INTRODUCTION

The seven TTAS's, produced by Symmetrics Corporation, were acquired by WSMR in 1967 with the first being delivered in 1969. (TTAS #1 is illustrated in Figure 2.) The TTAS is a self-contained, transportable, dual-axis telemetry tracking system using, originally, a single-channel monopulse antenna feed to automatically track a moving target transmitting an S-band or L-band telemetry signal with a minimum tracking threshold (receive level) of -120 dBm with a 100 kHz bandwidth. The tracking system can be slaved to externally derived pointing data (from a radar, for example) for initial target acquisition or reacquisition if it loses automatic track (called Autotrack), or it can be manipulated manually by an operator.

OVERVIEW OF THE PROTOTYPE TRACKING SYSTEM

The development of the new position control algorithm involved the characterization of the entire prototype tracking system using Laplace transforms and difference equations (z-transforms). (A block diagram describing one axis of the tracking system is illustrated in Figure 1.)

The Rate Loop

The understanding of a position control system begins with an understanding of its rate loop which contains the motor. The motor is characterized using the following three differential equations describing the motor-torque relationships as seen by the motor on its side of the gearbox:

$$T_M = j(d21e_M/dt^2) + B(d1_M/dt) + T_N \qquad (1)$$

$$T_M = K_i I_a \qquad (2)$$

$$E_a = RI_a + L(dI_a/dt) + K_b(d1_M/dt) \quad (3)$$

B = total viscous friction, as seen by motor
E_a = applied voltage to motor
I_a = motor current
J = total moment of inertia, as seen by motor
K_b = motor back emf constant
K_i = motor torque constant
L = armature inductance
T_M = torque produced by motor, on motor side of the gearbox
T_N = noise torque (considered negligible)
R = armature resistance
1_M = rotor position

From equations 1 and 2, tracking acceleration is proportional to the amount of available motor drive current and inversely proportional to the moment of inertia. For TTAS #1, the azimuth and elevation moments of inertia were measured (on the load side of the gearbox) to be approximately 1600 ft-lb-sec^2 and 325 ft-lb-sec^2 respectively. Thus, the azimuth tracking acceleration and deceleration are more limited than in elevation (because the motor drive current is also limited) and the azimuth stability margin is reduced.

The power amplifier, tachometer loop, and current loop are described with the next equation:

$$E_a = A\{E_i - K_tK_{att}(d1/dt) - f(I_a)\} \quad (4)$$

For the prototype tracking system, no nonscaler compensation is necessary in the forward part of the rate loop. Thus, the power amplifier gain in each axis is represented by the simple scaler gain constant A in the linear range of the power amplifiers. (The original amplifiers utilized lead-lag compensation.) Because the power amplifiers saturate, a nonlinear area is created in which a maximum limit is placed on tracking velocity, as indicated by equation 3. The tachometer feedback loop also uses scaler compensation--the tachometer constant (K_t) and attenuation (K_{att}). Current loop feedback is nonlinear--essentially, the magnitude of the current is squared. The result of limiting motor drive current is that the motor torque output is limited, as indicated by equation 2. This subsequently places a maximum

limit on tracking acceleration, as indicated by equation 1. (The purpose in limiting the motor drive current is to prevent the motor from overheating and to prevent the rotor windings from becoming distorted.)

Position Loop Compensation

The position control compensation selected for the prototype tracking system is the PID (proportionality-integrator-differentiator) controller illustrated in Figure 3. The pure integrator present in this compensation causes the prototype tracking system to be type-2. (The original position control compensation used a lossy integrator to create a type-1 control system-)

To implement the PID controller algorithm in the computer software, discrete z-domain (or difference) equations were used to represent it. After computing the PID drive output, the computer sends the output to the rate loop via a digital-to-analog converter (DAC) using the zero-order hold technique. Because it is possible for the PID controller to generate values exceeding the saturation level of the DAC, nonlinear compensation was incorporated into the PID controller algorithm to limit its maximum output to that of the DAC without changing its primary function of creating a type-2 tracking system. (DAC saturation is one of the more critical nonlinearities affecting tracking system control.)

The Manual, Slave, and Autotrack Position Feedback Paths

The prototype tracking system has two position feedback paths per axis. The first, used by the Manual and Slave tracking modes, is implemented through a coarse and fine synchro set and dual-speed synchro-to-digital converter (SDC, refer to Figure 1). The SDC provides 16-bit resolution or 19.8 seconds of arc making position deadband (or granularity) negligible. The computer then derives the tracking error by reading the encoder used by an operator in the Manual tracking mode or by reading the externally derived pointing angle data in the Slave tracking mode and subtracting the SDC data. (In the original tracking system, control and transmit synchros were used for Manual mode.)

The other position feedback path utilizes the RF subsystem in the Autotrack tracking mode, the main tracking mode. The

tracking error signals in Autotrack are derived by the conical scan feed, receivers, and tracking error demodulators. In this mode, the computer reads the tracking error an the receiver AGC output to determine whether the received signal is within the main beam of the antenna.

PROTOTYPE TRACKING SYSTEM RESULTS

Root Loci

Three root loci describe the frequency response of the prototype tracking system and are shown in Figures 4, 5, and 6. They were generated from a third-order characteristic equation and illustrate only the placement of the poles to show where the system is overdamped, critically damped, or underdamped. (The inclusion of the zeros into the root loci was unnecessary.)

The shape of the root locus is dependent on two of the PID controller gains (K_p and K_D) and the configuration of the rate loop, while location within a root locus is dependent only on the PID integrator gain, K_I In Figure 4, when K_p is not much bigger than K_D, the tracking system will be overdamped when K_I is small and become underdamped as K_I increases. As K_p increases relative to K_D the root locus in Figure 5 is generated showing that when K_I is small, the tracking system will be underdamped. As K_I increases, the tracking system becomes overdamped. However, as K_I continues, to increase, the tracking system again becomes underdamped, but less stable than when K_I was small initially. Finally, when K_p is much larger than K_D, the tracking system will always be underdamped regardless of the value of K_I as illustrated in Figure 6.

Of the three root loci, the PID gains creating the root locus illustrated in Figure 5 were selected as being the optimum gains for the prototype tracking system because they are the largest gains which allow the tracking system to be overdamped or critically damped and have better performance than the gains creating the root locus in Figure 4. An underdamped response is not acceptable, thus the gains creating the root locus in Figure 6 are not acceptable.

Computer Simulation Results

Computer simulation provided the least difficult means of studying the effects of the numerous nonlinearities present within the prototype tracking system. Current limiting and DAC saturation were discovered to be the most dominant nonlinearities of the tracking system, causing regions of instability to exist not predicted by the root loci because nonlinear stability is a function of the magnitude of tracking error.

Four basic servo tests were conducted using computer simulation to study the tracking performance of the prototype tracking system. These were the small step input, large step input, constant velocity input, and constant acceleration input tests. (The large step response was used to study nonlinear stability.) The position and tracking error results for each of these tests are illustrated in Figures 7, 8, 9, and 10 respectively.

Using the root locus results, gains for the PID controller were selected to achieve a critically damped response for low tracking bandwidth, as depicted by the small step response in Figure 7. Overshoot was minimized to about 12 percent and the settling time to 1.5 seconds. The large step response, in Figure 8, appears overdamped because of the nonlinear compensation which comes into action for large tracking errors. If the nonlinear compensation was removed, the large step response would be severely underdamped because the PID integrator will store very large values requiring much more time to settle. If either of these responses had been unstable, the position would have oscillated within a range not exceeding 10 degrees because the tracking system nonlinearities prevent the oscillation magnitude from exponentially increasing, as depicted by linear control theory. (This is also true of the actual tracking system.)

The constant velocity and constant acceleration responses illustrated in Figures 9 and 10 respectively prove that the prototype tracking system is type 2 because the steady-state constant velocity tracking error is zero and the steady-state constant acceleration tracking error is a non-zero constant. With the PID gains selected for these tests, a tracking system K_a of 15.6 was achieved.

Actual Prototype Tracking System Results

The following actual prototype tracking system tests were conducted on the azimuth axis and are the same type as done with the computer simulation. For each test, the same PID controller gains were used and were similar to those used for the computer simulation. The graphs illustrated were generated by the prototype tracking system computer. (The response information provided in the upper right-hand corner of each graph is not completely correct because the software used to generate the graphs was not complete at the time these graphs were printed.)

The first test was a one-degree small step response with a starting position of one degree as illustrated in Figure 11. The settling time was under 1.5 seconds. The overshoot was 100 percent because of the large moment of inertia in the azimuth axis. (The elevation axis experiences 25 percent overshoot for this test using similar PID gains.) Though the overshoot is high, the response is acceptable because the response was critically damped and settled quickly.

The 45-degree large step response from an initial position of five degrees, illustrated in Figure 12, was better than the computer simulation large step response illustrated in Figure 8. The large step settling time was approximately two seconds and the overshoot was about 3%. The overshoot is very small because the nonlinear compensation used in the control algorithm dominates the control of the response as with the computer simulation.

Figures 13 and 14 illustrate the azimuth axis velocity and tracking error respectively for a five degree/second constant velocity response. The tracking system reaches constant velocity in under two seconds and the steady-state tracking error is zero indicating that the prototype tracking system is not type-1.

Figures 15 and 16 illustrate the linearly-increasing velocity and tracking error for a 2-degree/second/second constant acceleration test for the azimuth axis. The prototype tracking system reaches a steady-state tracking error of about 0.17 degrees in less than two seconds meaning that the K_a for this test was approximately 12 and that the prototype tracking system is type-2.

COMPARISON WITH THE ORIGINAL TRACKING SYSTEM

The tracking performance of the original type-1 tracking system is illustrated using a computer simulation constant velocity and constant acceleration response shown in Figures 17 and 18 respectively.

For a constant velocity input, the type-1 tracking system has a non-zero steady-state tracking error; and for a constant acceleration input, there is no steady-state tracking error. K_a is zero. Thus, the original type-1 tracking system cannot, for extended periods of time, track a constantly accelerating target because the tracking error eventually exceeds the beamwidth of the antenna and loses Autotrack. In contrast, the prototype type-2 tracking system could, theoretically, track a constantly accelerating target indefinitely; but the actual tracking system would reach maximum velocity, a pedestal travel limit, or both.

PROBLEMS ENCOUNTERED WITH THE TRACKING SYSTEM

Several problems were discovered with the TTAS directly affecting the prototype tracking system after its installation in the TTAS. Two of the problems and their solutions are discussed below.

Chaotic Synchro-to-Digital Converter Behavior

The synchro-to-digital converters used in the TTAS, not part of the installed prototype tracking system equipment, are a dual-speed converter set consisting of two interconnected modules. At random times, the SDC’s report erroneous pedestal positions to the prototype tracking system computer. If the computer is in the Manual or Slave tracking mode at that time, it interprets the reported erroneous positions as being actual and attempts correction. This results in the pedestal suddenly jerking forward and immediately returning to the prior correct position because the erroneous position data is usually reported during only one iteration. Repeated severe jerking eventually caused the azimuth gearbox to be torn loose within the pedestal and required repair.

During the exhaustive investigation which isolated this problem to the SDC’s, the SDC manufacturer was contacted and

asked for assistance to identify the cause of the problem. The manufacturer identified the problem as an inherent design flaw within the converters, for which the only the solution is replacement. As a temporary solution, before the replacement SDC's are acquired, software was written to recognize the position feedback spikes and prevent them from entering the position loop. Spikes of small magnitude are not suppressed by this software, but their potential to damage the pedestal is very small.

Tracking Error Signal Noise

The tracking error demodulators, acquired with the conical scan feed, output tracking error signals comprised of about 50 percent ac ripple at the conical scan rate frequency and other high frequency noise. Because the prototype tracking system computer samples data at a slower rate than the conical scan frequency, it was necessary to add analog filtering to the tracking error demodulator outputs to prevent the tracking error signal noise from entering the position control loop. The inclusion of the analog filtering in the Autotrack position feedback reduced the gain and phase margins of the tracking system. To accommodate for the altered response, the PID gains were modified to compensate for the increased lag from the analog filtering.

CONCLUSION

The incorporation of the computer controlled prototype tracking system into the TTAS has thus far proven to be an excellent replacement for the increasingly cumbersome analog control system. The dynamic capability of the tracking system has been enhanced by the type-2 PID algorithm, and through the self-diagnostic software and automated test system developed for the computer controller, TTAS operators will be able to quickly identify problems within the TTAS and measure various system parameters such as the system K_a, G/T, antenna pattern, and noise floor. Also, the incorporation of that computer has provided a future capability of controlling the TTAS remotely. (The original control system has no remote control capability.) Thus, the use of digital technology in the place of classic analog servo components for future telemetry tracking system designs has been shown to offer numerous advantages and performance improvements.

An identified possible potential problem with the prototype tracking system will be the longevity and durability of the computer equipment housed in a mobile van in a field environment. The imminence of this problem is not yet known.

ACKNOWLEDGEMENTS

Other members of the team which developed the computer controlled telemetry tracking system included the following White Sands Missile Range personnel:

Phillip D. Sharp	Henry B. Stephenson, Jr.	Marcelo V. Rosales
Moises Pedroza	James E. Tillett	Ted A. Marsh
Mark C. Ehlers	Daniel C. Bissell	James W. Cutler, Jr.
Vaughn L. Bourget		

REFERENCES

Jacquot, Raymond G., Modern Digital Control Systems. New York, New York: Marcel Dekker, Inc.,1981.

Kuo, Benjamin C., Automatic Control Systems, Fourth Edition. Englewood Cliffs, New Jersey: Prentice-Hall, Inc., 1982.

Phillips, Charles L. and Harbor, Royce D.; Feedback Control Systems. Englewood Cliffs, New Jersey: Prentice-Hall, Inc., 1988.

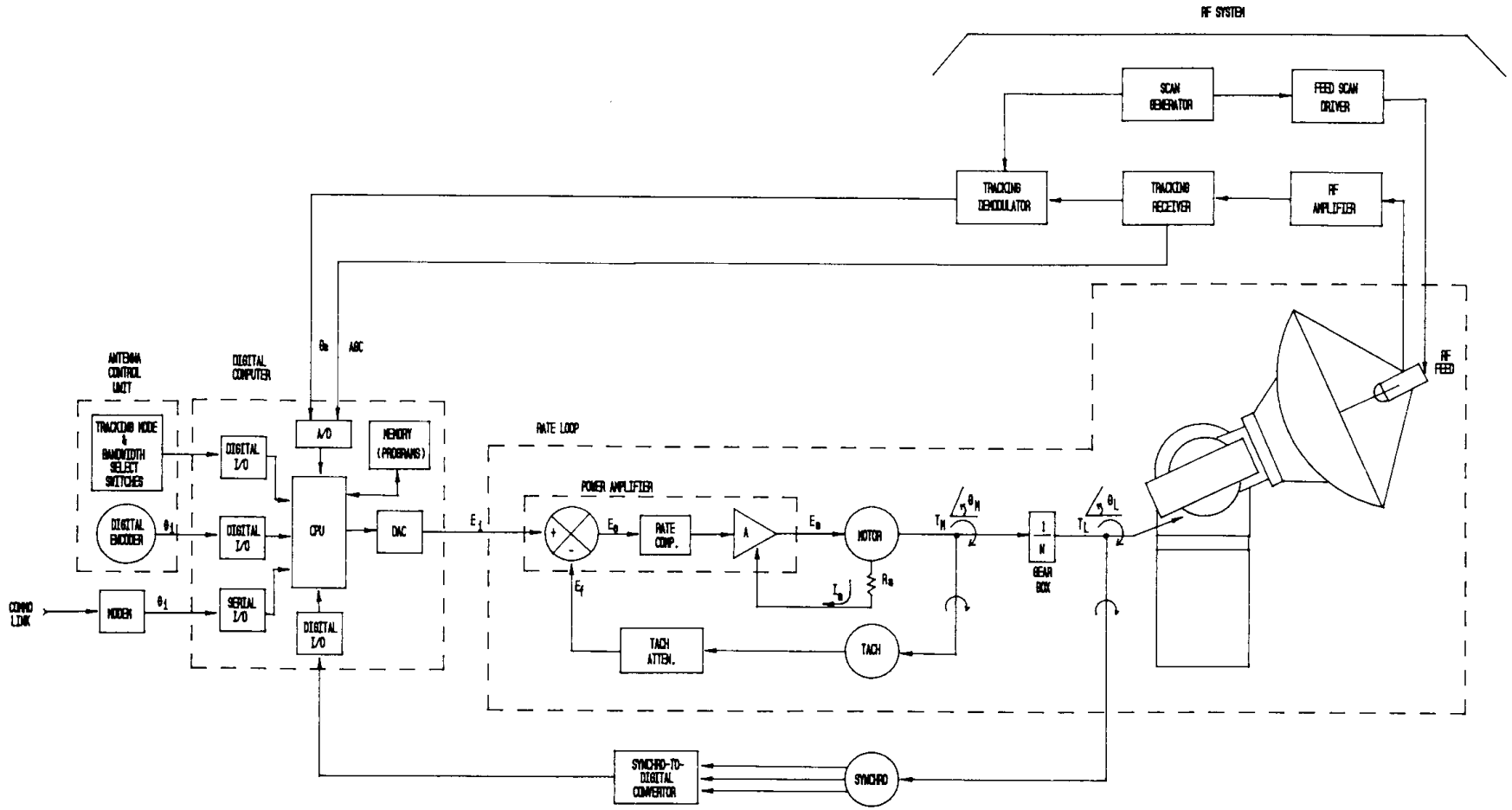

Figure 1. PROTOTYPE TRACKING SYSTEM BLOCK DIAGRAM
(One Axis)

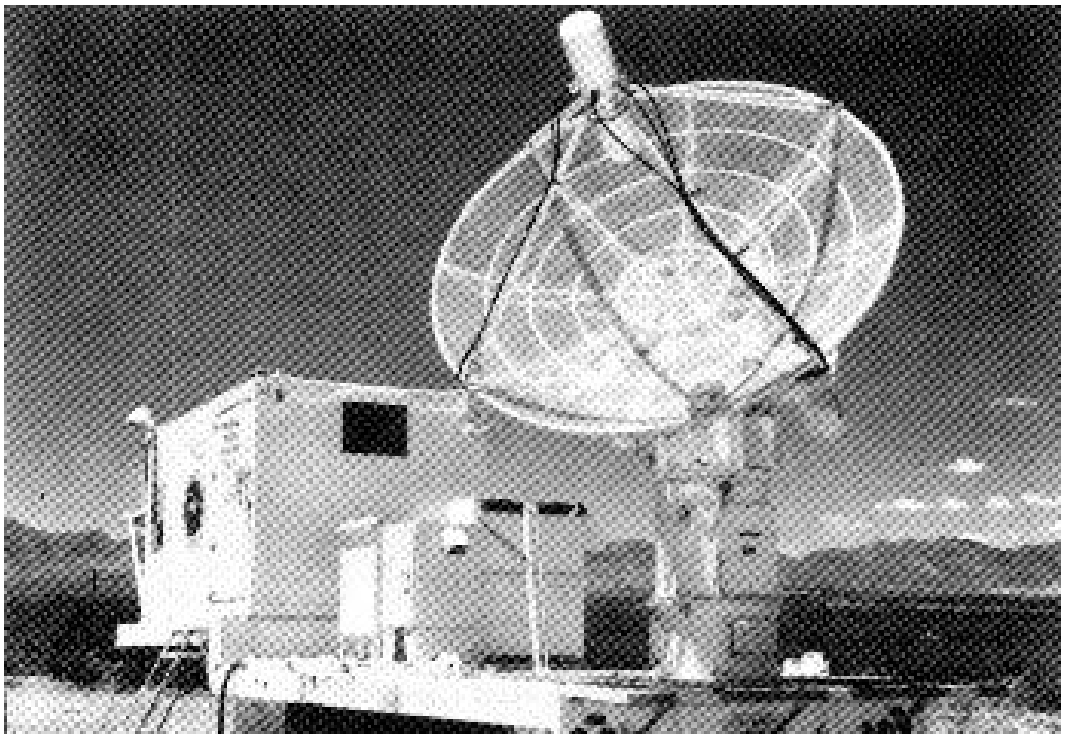

Figure 2. Photograph of TTAS #1

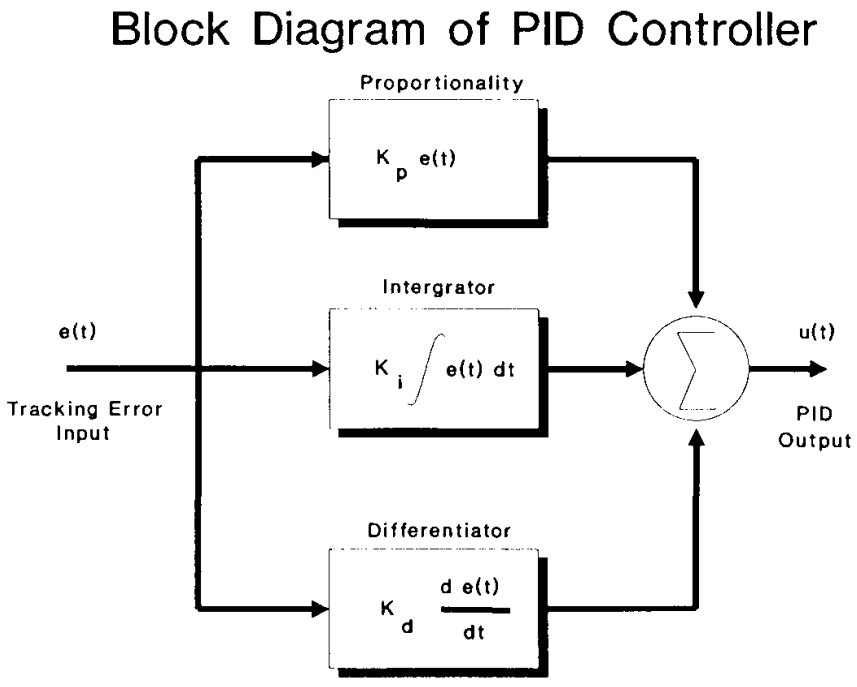

Figure 3

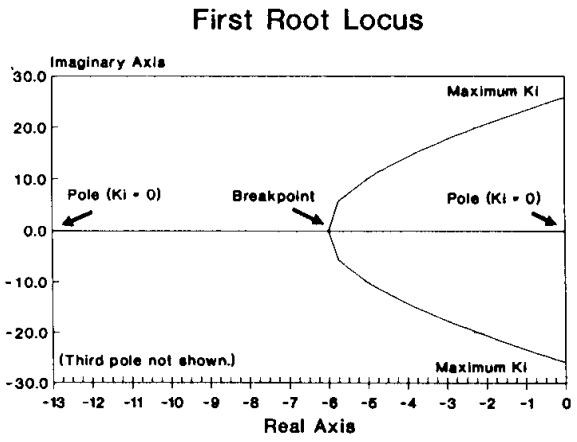

Figure 4

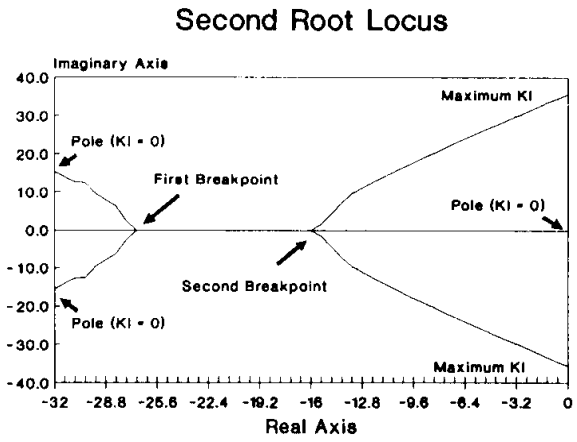

Figure 5

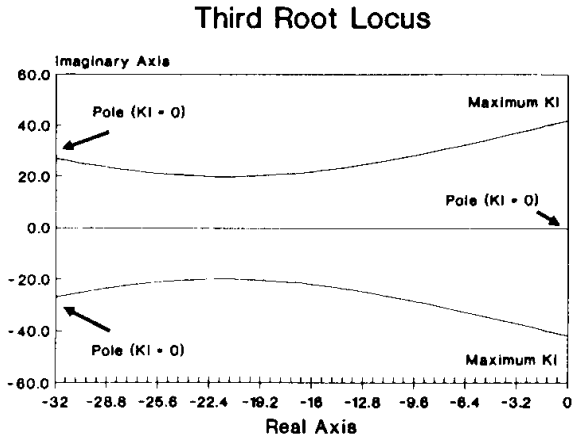

Figure 6

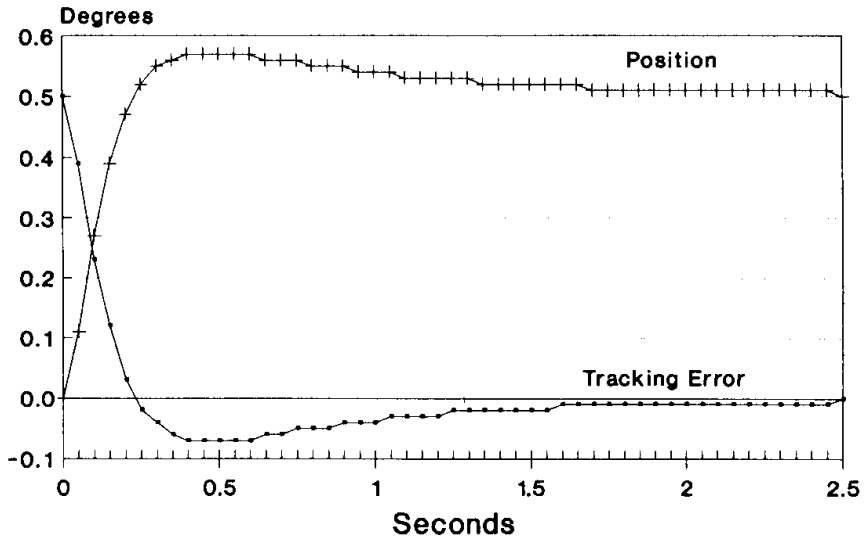

Figure 7

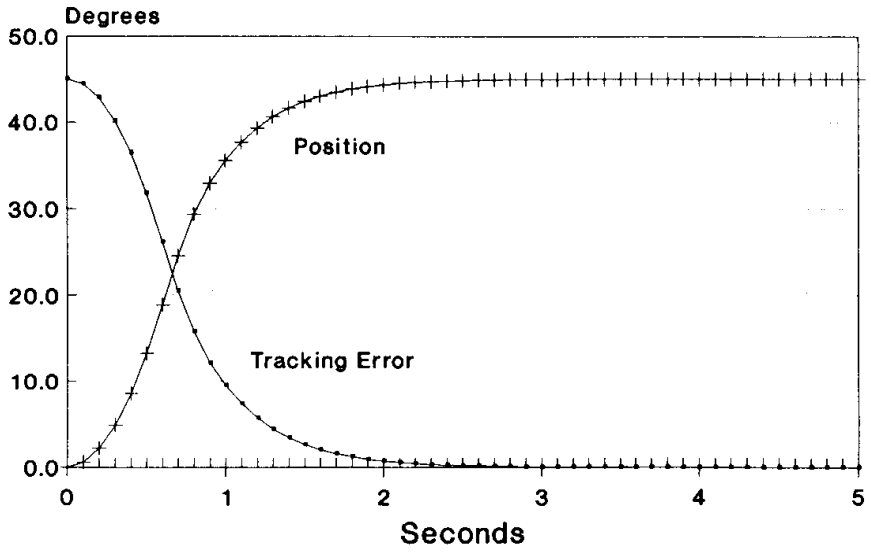

Figure 8

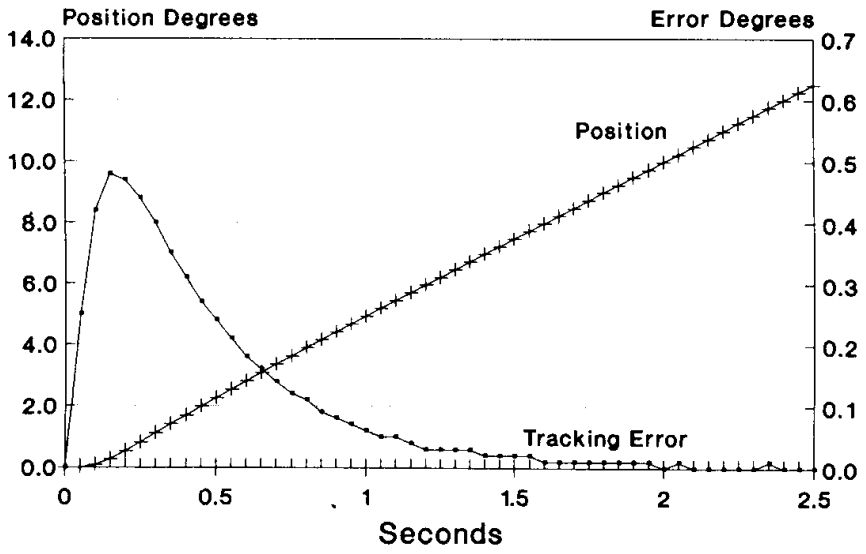

Figure 9

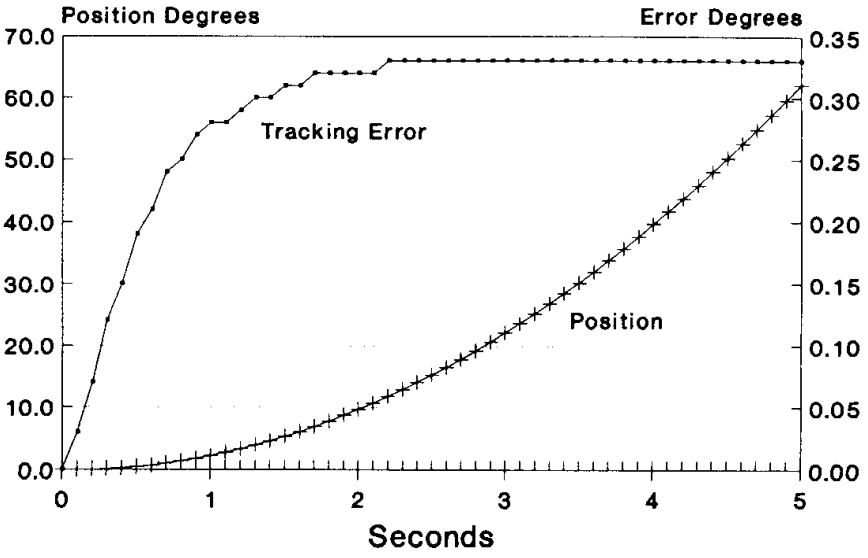

Figure 10

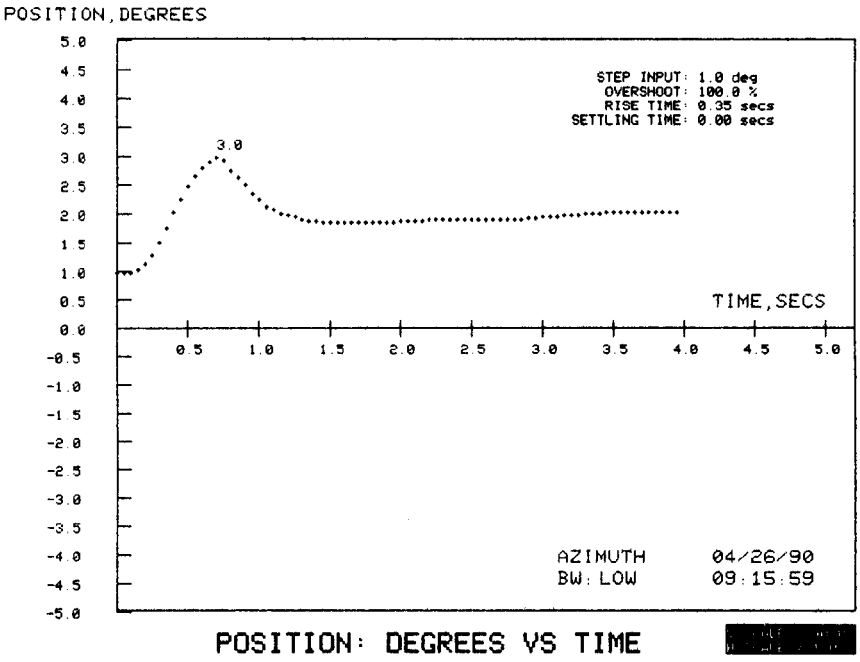

Figure 11. Small Step-Response

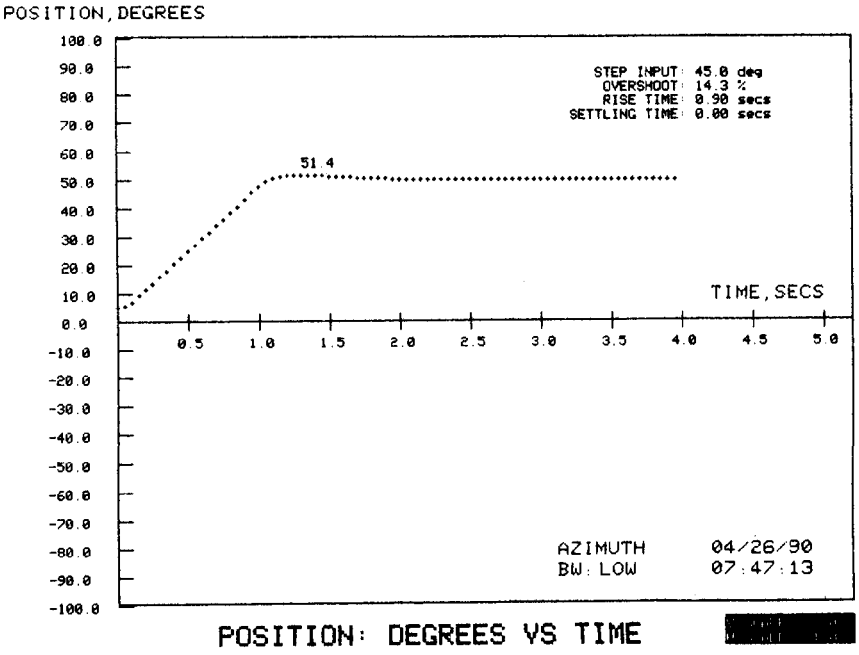

Figure 12. Large Step Response

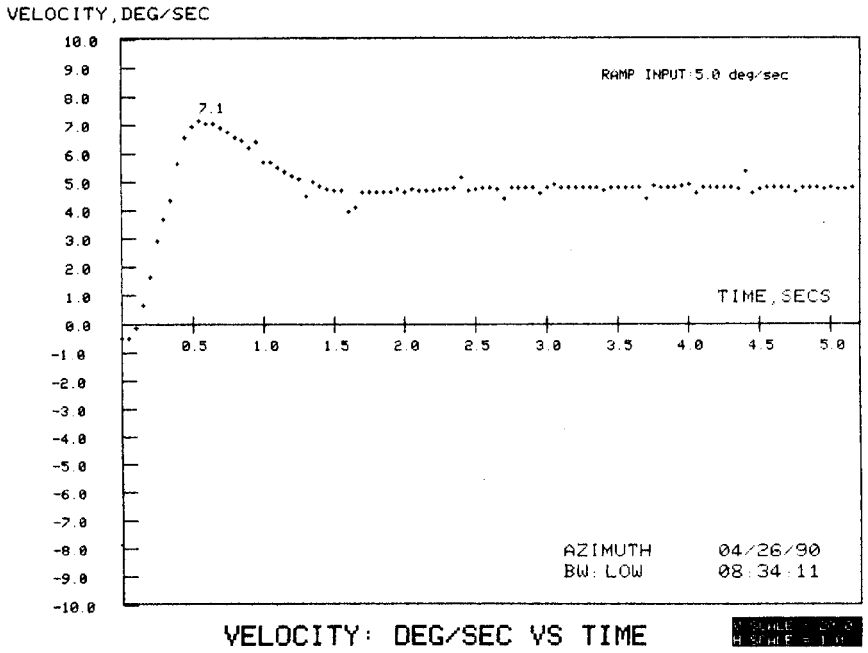

Figure 13. Constant Velocity Response, Velocity

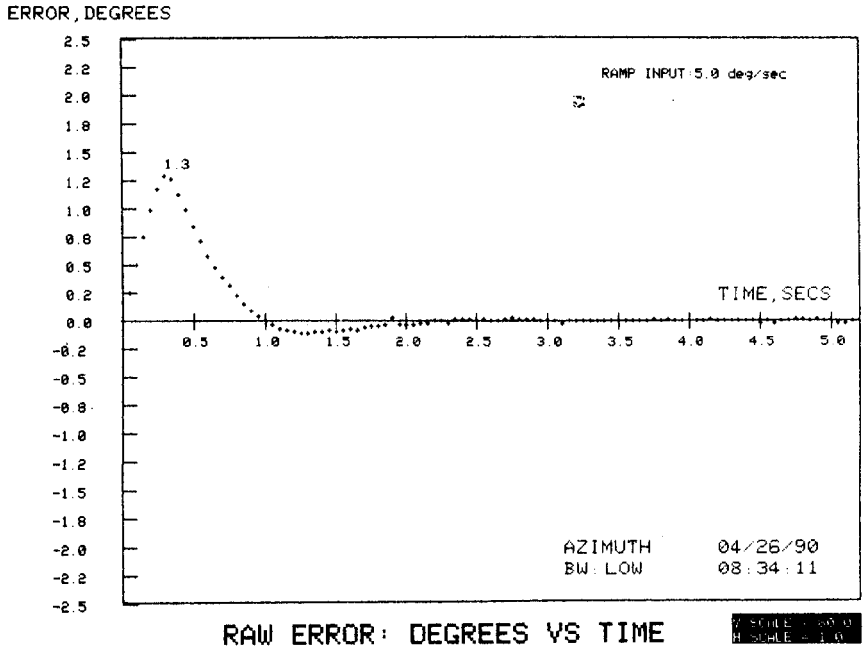

Figure 14. Constant Velocity Response, Tracking Error

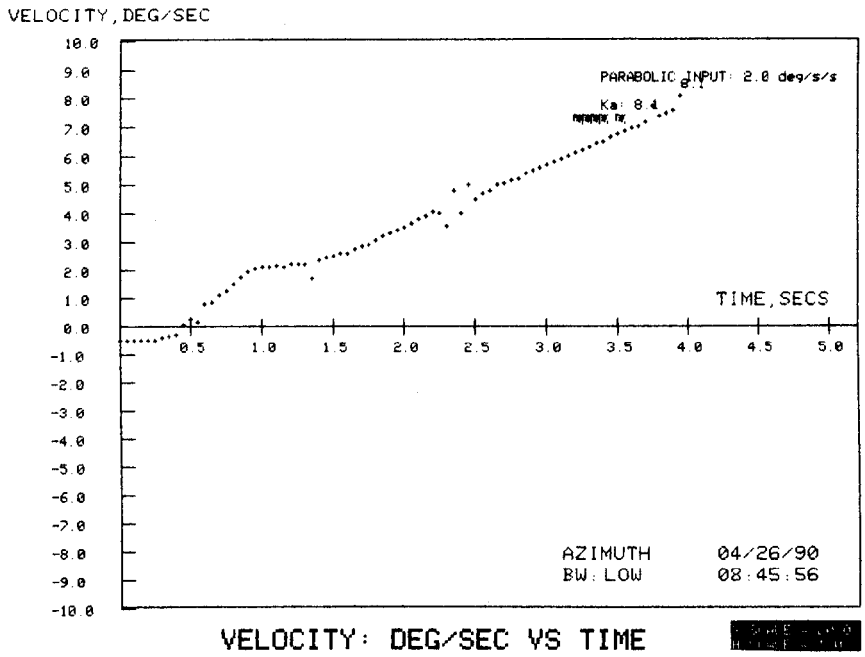

Figure 15. Constant Acceleration Response, Velocity

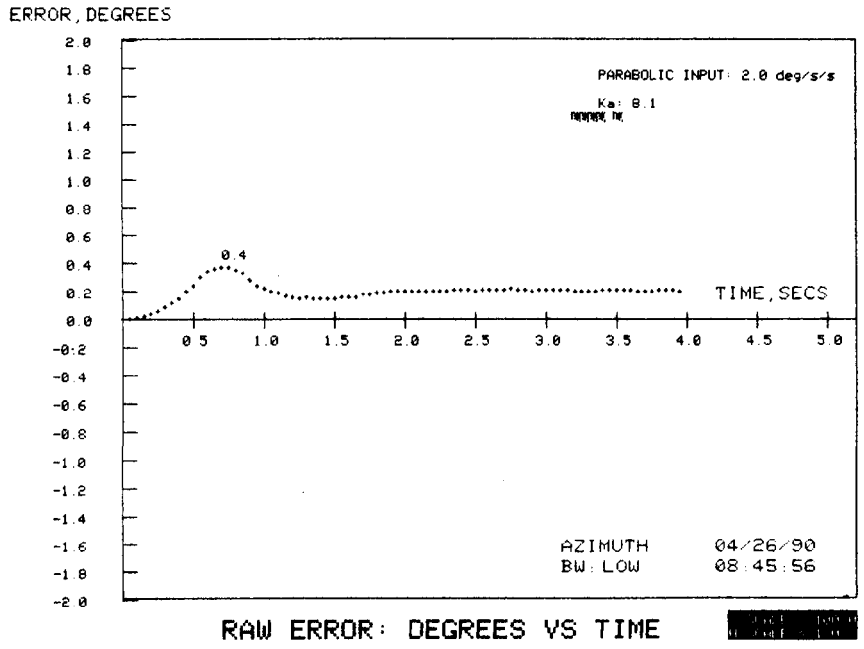

Figure 16. Constant Acceleration Response, Tracking Error

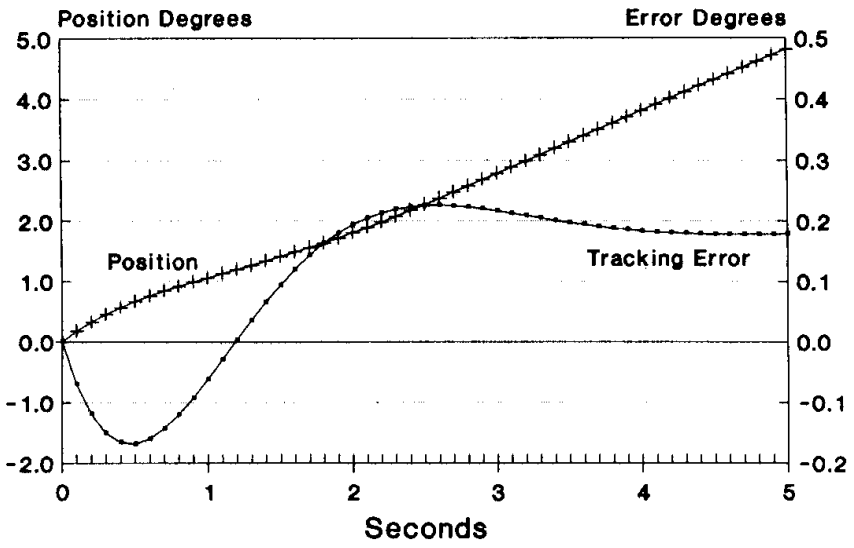

Figure 17

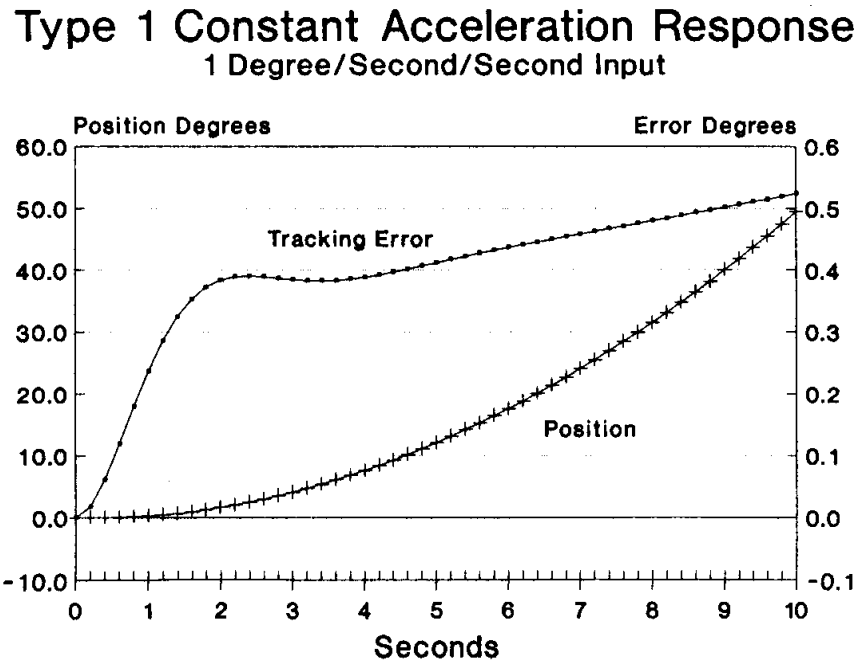

Figure 18